Semiconductor-quasimetal transition of heavily doped *trans*-polyacetylene

Manfred Dinter
I. Institut für Theoretische Physik, Fachbereich Physik, Universität Hamburg, Jungiusstrasse 9, D-2000 Hamburg 36, Federal Republic of Germany
(Received 6 September 1988)

Within the continuum models of Takayama, Lin-Liu, and Maki and of Brazovskii and Kirova, a new doping-induced superlattice form has been found to exist on chains of conducting polymers with zero confinement. It has smaller total energy than the soliton lattice of Horovitz and has properties which can help remove existing discrepancies between theory and experiment. The dependence of electronic band energies, density of states, and static magnetic susceptibility on dopant concentration is shown. Results are compared to those from the soliton lattice. In the quasimetallic state delocalized band states coexist with localized charges in absence of a band gap.

I. INTRODUCTION

Interest in conducting polymers has grown in recent years, in part due to their novel features in form of nonlinear excitations, which have become known under the names solitons,[1,2] polarons,[3,4] and bipolarons.[5,6] Two theoretical microscopic models have successfully been applied in this context. The discrete coupled equations of Su, Schrieffer, and Heeger (SSH) (Ref. 7) or their continuum counterpart of Takayama, Lin-Liu, and Maki (TLM),[8] and the model of Brazovskii and Kirova (BK),[9] which lifts the twofold degeneracy of the ground state so that it can be used for a wider class of polymers, of which *cis*-polyacetylene, polyparaphenylene, polypyrrole, and polythiophene are well-known examples. Results for low concentration are comparable to those of numerical work.[10,11]

With growing dopant concentration the distance between these excitations decreases and they interact to form superlattices. Experiment supports this point of view. Spectroscopic methods reveal that at least in the crystalline part of the material doping proceeds in steps accompanied by three-dimensional structural reordering. Columns of dopant ions with regular spacing between the ions intercalate with host polymer chains, on which the transferred excess charges are localized in a pattern following the dopant array.[12–16] Within the framework of the one-dimensional TLM and BK models, theory predicts soliton[17,18] and (bi)polaron lattices.[19,20] Many experiments, for example, electron-spin resonance and electromagnetic absorption, can be interpreted in terms of spinless solitons or bipolarons depending on whether the material's confinement parameter Δ is zero or not. At still larger concentrations of dopants many polymers more and more become metalliclike. The difficult problem of the high electrical dc conductivity set aside, phenomena such as an enhanced Pauli spin susceptibility must be understood,[21–23] and the narrowing or vanishing of the band gap in optical absorption[11,14,24] has to be explained, as well as the persistance of doping-induced infrared-active vibrations characteristic of localized charges to highest dopant levels.[24,25] To this end Kivelson and Heeger[26] proposed a crossover from a soliton (or bipolaron) lattice to a polaron lattice with half-filled upper (or lower) localization band at a critical concentration, where the separation between solitons becomes comparable to their width. However, apart from the sensibility of such a transition towards small energy contributions from interchain hopping, electron correlation, quantum fluctuations, and disorder, it has been shown[27] in a one-dimensional calculation that infrared modes should be unobservable in a polaronlike lattice at high concentration, contradictory to experiment.[24,25]

In view of the complexity of the problem many questions arise, one of wich is whether the solutions of the TLM and BK equations known to date are sufficiently general to help explain all known experiments. It will be shown in this paper that this is, in fact, not the case, with an example for zero confinement. Reference 26 relies on the soliton lattice having the lowest total energy for small and intermediate doping. But there exists another lattice form with even smaller energy and with properties that could remove discrepancies with experiment. This solution is encountered when studying the self-consistency equations of Ref. 20 for partially filled localization bands in the limit $\Delta=0$. These equations allow for a wide variety of occupying gap states on finite polymer chains at any doping level. We explore the particular but obvious case of a fractionally filled band, thus generalizing the details of Ref. 26. The dependence on confinement energy Δ shall be investigated in another paper. Although we are here concerned with $\Delta=0$ aiming at a description of *trans*-polyacetylene, we first establish the equations for the general case. This will be done in Sec. II. Section III is devoted to the derivation of formulas for the dependence of electronic band structure and density of states on dopant concentration. Results for $\Delta=0$ will be found in Sec. IV, which compares the new superlattice to the soliton lattice with respect to shape, wave function, density of states, band structure, and susceptibility. Discussion of the results and further conclusions follow in Sec. V.

 ©1989 The American Physical Society

II. SUPERLATTICE WITH PARTIALLY FILLED LOCALIZATION BAND

Without loss of general validity the discussion can be restricted to the case of n-type doping, where the valence and lower localization band are full by assumption, but the upper band of localized states is only partially filled. We introduce a filling factor Q with $Q \leq 1$. Under neglection of even-odd effects considered in Eq. (16) of Ref. 20, the set of quantum states ν (generalized wave numbers) decomposes into localized states $-n/2 \leq \nu \leq n/2$ and extended states $\nu = \pm n/2, \ldots, \pm N/2$. Here n denotes the number of superlattice dips and N the number of monomers on the chain. Figure 1 makes the meaning of Q concise. Evidently, $n' = nQ$ is the number of electron pairs transferred upon doping. Let us define two variables: $c = n/N$, the fraction of superlattice wells on the chain with $0 \leq c \leq 1$, and $y = n'/N$, the fraction of charge pairs. An immediate consequence is the relation $y = Qc$ with $0 \leq y \leq Q$. At $y > Q$ either the filled fraction Q of the old superlattice increases, or there is a phase transition to a superlattice with larger n. y is proportional to the dopant concentration y_D, the total number of excess charges divided by the total number of carbon atoms on the chain. Polyacetylene, for example, has $y = 2y_D$. At constant y one can envision phase transitions between different c with $Q \sim 1/c$, from a full band ($Q = 1$) with a minimal number of superlattice cells to $Q = y$ with a maximal cell number. Their relative stability remains to be studied.

The function $n_{+\nu} - n_{-\nu}$ is substantial for the self-consistency conditions, Eqs. (18), of Ref. 20. Here $n_{\pm\nu}$ are occupation numbers of quantum state ν in the upper (lower) localization bands. The present paper deals with twofold occupied levels, which means $n_{+\nu} - n_{-\nu} = 0$ for $0 \leq |\nu| < Qn/2$ and $n_{+\nu} - n_{-\nu} = -2$ for $Qn/2 \leq |\nu| < n/2$. For not too small n and N, the ν sums of Ref. 20 can be converted to integrals. Both self-consistency equations then read

$$\frac{1}{\lambda}\left[1 - \frac{2\Delta}{G}\right] = \frac{\pi}{n}\int_{n/2}^{N/2} d\nu \frac{k^2 + (k/\alpha_\nu)^2}{[(1 + k^2/\alpha_\nu^2)K - E][M + k^2 + (k/\alpha_\nu)^2]^{1/2}} + \frac{\pi}{n}\int_{Qn/2}^{n/2} d\nu \frac{(k/\beta_\nu)^2 - k^2}{[E - (1 - k^2/\beta_\nu^2)K][M + k^2 - (k/\beta_\nu)^2]^{1/2}},$$

$$\frac{1}{\lambda}\frac{2\Delta}{G}\frac{1}{M} = \frac{\pi}{n}\int_{n/2}^{N/2} d\nu \frac{1}{[(1 + k^2/\alpha_\nu^2)K - E][M + k^2 + (k/\alpha_\nu)^2]^{1/2}} - \frac{\pi}{n}\int_{Qn/2}^{n/2} d\nu \frac{1}{[E - (1 - k^2/\beta_\nu^2)K][M + k^2 - (k/\beta_\nu)^2]^{1/2}}, \tag{1}$$

where λ is the dimensionless electron-phonon coupling constant (for polyacetylene $\lambda = 0.38$, for polydiacetylene $\lambda = 0.43$), and Δ is the confinement parameter,[6] which is zero for *trans*-polyacetylene, 0.12 eV for *cis*-polyacetylene, and 0.19 for polydiacetylene, for example. The function M has been introduced in Eq. (9) of Ref. 20. It can be put into a more practical form,

$$(M + k^2)(M + k^2 - 1)/M = \left[\frac{G}{2v_F\kappa}\right]^2 = \left[\frac{\pi G}{2ScK(k)}\right]^2. \tag{2}$$

The special choice of M reproduces all superlattice solutions known today as the soliton,[1,2] polaron,[3,4] and bipolaron.[5,6] The auxiliary functions α_ν and β_ν are explained in Eqs. (17) of Ref. 20. They are generalized phase shifts of wave functions. The gap parameter G is not a constant, but depends on c, and is implicitly determined by Eqs. (1). So is the modulus k ($0 \leq k \leq 1$), which is responsible for the shape of the superlattice. The total bandwidth $S = 2\pi v_F/a$ is about 10 eV for polyacetylene and 8.4 eV for polydiacetylene. κ measures gradients and $\kappa = 2nK(k)/Na$, as has been found in Eq. (12) of Ref. 20 from the requirement of periodicity. v_F and a are Fermi velocity and monomer length, respectively. Results from the continuum models (TLM, BK) are valid as long as

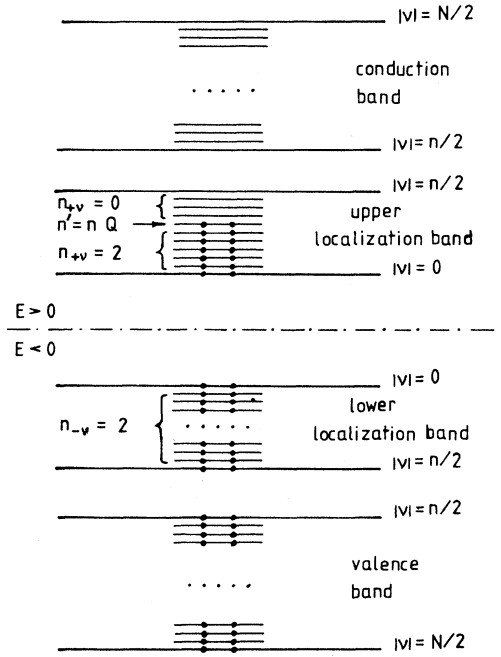

FIG. 1. Occupation of band states. Localized states: $-n/2 \leq \nu \leq n/2$. Delocalized states: $\nu = \pm n/2, \ldots, \pm N/2$. N number of monomers on chain. n number of superlattice dips. $2n'$ number of excess charges. $Q = n'/n \leq 1$ fraction of possible localized states occupied by excess charges, shown here for the case of doping with negative charges.

$a\kappa \ll \pi$ or, equivalently, $cK(k) \ll \pi/2$. The integrals of Eqs. (1) are calculated in Appendix A, leading to a coupled system of equations (A8), which determine the parameters k and G in terms of c and Q.

We still are in need of an expression for the total energy W, which can serve as a criterion for relative stability, and which in our case comprises electronic and lattice contributions. It is given in Eq. (19) of Ref. 20. Its integral approximation reads

$$W=\int_{-Na/2}^{Na/2} dx \frac{(\tilde{\Delta}-\Delta)^2}{S\lambda a} - 2v_F\kappa \int_{n/2}^{N/2} d\nu [M+k^2+(k/\alpha_\nu)^2]^{1/2} - 2v_F\kappa \int_{Qn/2}^{n/2} d\nu [M+k^2-(k/\beta_\nu)^2]^{1/2} . \quad (3)$$

The lattice configuration function $\tilde{\Delta}$ can be found from Eqs. (7) and (8) of Ref. 20 by use of the Jacobian elliptic functions sn, cn, and dn:

$$\tilde{\Delta}(x)=\frac{MG/2+v_F\kappa k^2 \mathrm{sgn}(x_0)\mathrm{sn}[\kappa(x-x_0),k]\mathrm{cn}[\kappa(x-x_0),k]\mathrm{dn}[\kappa(x-x_0),k]}{M+k^2\mathrm{cn}^2[\kappa(x-x_0),k]} . \quad (4)$$

It describes the atomic displacement along the polymer chain. This solution of the nonlinear continuum model is sufficiently general to reproduce all superlattice forms known to date. The special choice

$$2\kappa x_0 = F\left[\sin^{-1}\frac{1}{(M+k^2)^{1/2}}, k\right] , \quad (5)$$

for x_0 yields the bipolaron solution Eq. (11) of Ref. 20. Inserting $\tilde{\Delta}$ into the first integral of Eq. (3) above and shifting $x \to x+x_0$, which does not change the integration boundaries on account of periodicity, we obtain[28]

$$\int_{-Na/2}^{Na/2} dx \frac{(\tilde{\Delta}-\Delta)^2}{S\lambda a} = \frac{N}{\lambda S}\left[\Delta^2 - G\Delta\frac{M}{M+k^2}\frac{1}{K(k)}\Pi(k^2/(M+k^2), k) + (v_F\kappa)^2[M+1-2E(k)/K(k)]\right] . \quad (6)$$

Application of operations Eqs. (A2)–(A5) to the other integrals of Eq. (3) gives the following result for the total energy per monomer:

$$\frac{W}{N}=\frac{1}{\lambda S}\left[\Delta^2+\tfrac{1}{2}G\Delta\frac{M}{M+k^2}-G\Delta\frac{M}{M+k^2}\frac{1}{K(k)}\Pi(k^2/(M+k^2), k) + \frac{G^2}{4S}\frac{\sqrt{M}}{M+k^2-1}\left\{\frac{M}{M+k^2}\left[E(\sin^{-1}X, k'(1+k^2/M)^{1/2}) - E\left[\sin^{-1}\left[\frac{1-\tilde{\beta}^2}{1-k^2}\right]^{1/2}, k'(1+k^2/M)^{1/2}\right]\right] - \frac{\{X^2(1-X^2)[1-(k')^2X^2(1+k^2/M)]\}^{1/2}}{1-(1+k^2/M)X^2} + \frac{\{(1-\tilde{\beta}^2)(\tilde{\beta}^2-k^2)[\tilde{\beta}^2(1+k^2/M)-k^2/M]\}^{1/2}}{\tilde{\beta}^2(1+k^2/M)}\right\}\right] . \quad (7)$$

W implicitly varies with c and Q. The chemical potential for the addition of a single charge can be received from the slope of W via

$$\mu=(2Q)^{-1}\frac{d(W/N)}{dc} .$$

III. ELECTRONIC DENSITY OF STATES AND ENERGY BANDS

The density of states per eV and carbon atom is computed in the usual way,

$$Z(E)=\frac{4}{N_C}\frac{d|\nu|}{d|E|}=\frac{4}{N_C}\frac{d|\nu|}{d\beta_\nu}\frac{1}{d|E|/d\beta_\nu} , \text{ etc.} \quad (8)$$

Here N_C is the number of carbon atoms on the chain and the factor 4 takes account of spin and both signs of ν. According to Eqs. (17) of Ref. 20 there are different formulas which describe localized and extended states:

$$|\nu|=\frac{n}{2}\Lambda_0\left[\sin^{-1}\left[\frac{\beta_\nu^2-k^2}{\beta_\nu^2(1-k^2)}\right]^{1/2}, k\right]$$

$$|E|=v_F\kappa[M+k^2-(k/\beta_\nu)^2]^{1/2} ,$$

for localized states and (9)

$$|\nu|=\frac{n}{\pi}\left[\frac{(1+\alpha_\nu^2)(k^2+\alpha_\nu^2)}{\alpha_\nu^2}\right]^{1/2}\Pi(-\alpha_\nu^2, k) ,$$

$$|E|=v_F\kappa[M+k^2+(k/\alpha_\nu)^2]^{1/2}$$

for extended states. $Z(E)$ consequently decomposes into contributions from the two localized and the two extended bands

$$S\frac{N_C}{4N}Z^{\rm loc}(E) = |\varepsilon|\frac{E(k)/K(k)+M+k^2-1-\varepsilon^2}{[(M+k^2-\varepsilon^2)(M-\varepsilon^2)(\varepsilon^2-M-k^2+1)]^{1/2}}\ ,$$

$$S\frac{N_C}{4N}Z^{\rm ext}(E) = |\varepsilon|\frac{\varepsilon^2-M-k^2+1-E(k)/K(k)}{[(\varepsilon^2-M-k^2)(\varepsilon^2-M)(\varepsilon^2-M-k^2+1)]^{1/2}}\ , \tag{10}$$

where $\varepsilon=E/v_F\kappa$. As is to be expected, Van Hove singularities mark the band edges. Obviously the latter are

$$E_l^{\rm cond}=v_F\kappa(M+k^2)^{1/2}=\frac{G}{2}\left[\frac{M}{M+k^2-1}\right]^{1/2}$$

for the lower boundary of the conduction band,

$$E_u^{\rm loc}=v_F\kappa\sqrt{M}=\frac{G}{2}\frac{M}{[(M+k^2)(M+k^2-1)]^{1/2}} \tag{11}$$

for the upper boundary of the band of antibonding localized states, and

$$E_l^{\rm loc}=v_F\kappa(M+k^2-1)^{1/2}=\frac{G}{2}\left[\frac{M}{M+k^2}\right]^{1/2}$$

for the lower boundary of the latter.

Use has been made of Eq. (2). The upper edge of the conduction band does not sensitively depend on doping and has been left out. The energies of lower localized and valence bands are mirror images of those given in Eqs. (11). Below we shall sketch the variation of band-edge energies with dopant concentration instead of showing the wave-vector dependence of E on the whole.

IV. RESULTS FOR ZERO CONFINEMENT $\Delta=0$

Because of the immense amount of work on *trans*-polyacetylene and its importance, the present discussion is restricted to the particular case $\Delta=0$. The investigation of $\Delta\neq0$ is deferred to another paper. Above equations are considerably simplified in the case of $\Delta=0$. The objection of why not use this condition right from the beginning and avoid the complications associated with Eqs. (A8) is not justified because that way a new superlattice solution could easily escape notice. The fourth of Eqs. (A8) reveals the existence of two solutions in the case of $\Delta=0$. One has $G=0$; the other $X=[(1-\tilde{\beta}^2)/(1-k^2)]^{1/2}$. The first is related to the well-known soliton lattice widely discussed in the literature.[17,18] The second is completely new and, as shown below, important.

Case (a): $G=0$. We conclude from the fifth of Eqs. (A8)

$$M=1-k^2\ . \tag{12}$$

Equation (4) yields the lattice function $\tilde{\Delta}$ for that case. It is even in x, if $x_0=Na/4n$, and odd, if $x_0=0$, where without loss of general validity we may assume $x_0>0$,

$$\tilde{\Delta}(x)=v_F\kappa k^2\frac{\mathrm{sn}[\kappa(x-x_0),k]\mathrm{cn}[\kappa(x-x_0),k]}{\mathrm{dn}[\kappa(x-x_0),k]} = v_F\kappa\frac{k^2}{1+k'}\mathrm{sn}[(1+k')\kappa(x-x_0),(1-k')/(1+k')]\ , \tag{13}$$

using Landen's transformation.[28] This is the soliton lattice known from the literature.[18] From Appendix B we infer $Q=1$ to yield the most stable state. In this case modulus k and total energy W/N are related to concentration y via

$$y=\frac{(\pi/2)\tanh(1/\lambda)}{[1+k^2\sinh^2(1/\lambda)]^{1/2}\Pi(-1/\sinh^2(1/\lambda),k)}\ ,$$
$$W/N=-\frac{S}{4}\frac{k^2\sinh^2(1/\lambda)}{1+k^2\sinh^2(1/\lambda)}\tanh(1/\lambda) \times\left[\frac{K(k)}{\Pi(-1/\sinh^2(1/\lambda),k)}\right]^2\ . \tag{14}$$

For later purposes we need the electronic density of states. $M=(k')^2$ reduces Eqs. (10) to

$$S\frac{N_C}{4N}Z^{\rm loc}(E)=\frac{E(k)/K(k)-\varepsilon^2}{\{(1-\varepsilon^2)[(k')^2-\varepsilon^2]\}^{1/2}}\quad\text{for } |\varepsilon|<k'\ ,$$
$$S\frac{N_C}{4N}Z^{\rm ext}(E)=\frac{\varepsilon^2-E(k)/K(k)}{\{(\varepsilon^2-1)[\varepsilon^2-(k')^2]\}^{1/2}}\quad\text{for } |\varepsilon|>1\ , \tag{15}$$

and zero elsewhere. See Fig. 2. Z is normalized to 1:

$$\frac{N_C}{4N}\int_{-S/2}^{S/2}dE\,Z(E)=1\ . \tag{16}$$

As is evident from Eq. (13), $\tilde{\Delta}$ vanishes near gap closure in the limit $k=0$; Z becomes a constant for all E: $(N_C/4N)Z(E)=1/S$. From Eq. (16), we compute

$$(N_C/4N)\int_0^{v_F\kappa k'}dE\,Z^{\rm loc}(E)=y/2\ .$$

That is to say that the Fermi energy $E_F=k'v_F\kappa=Syk'K(k)/\pi$ coincides with $E_u^{\rm loc}$ for all k, as

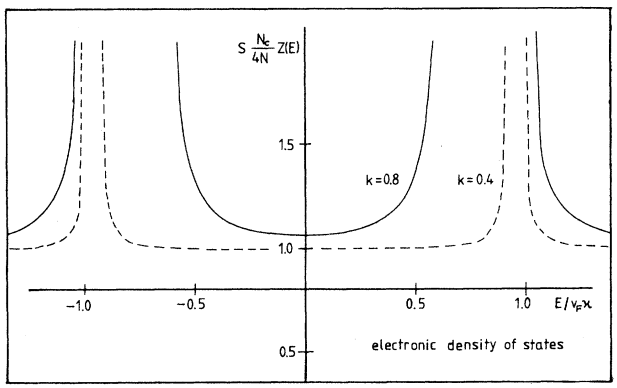

FIG. 2. Electronic density of states for soliton lattice with $Q=1$. Two values for modulus k. $k=0.4$ (dashed line); $k=0.8$ (solid line).

is to be expected for $Q=1$.

Case (b): $X=[(1-\tilde{\beta}^2)/(1-k^2)]^{1/2}$. We insert $X=[(1-\tilde{\beta}^2)/(1-k^2)]^{1/2}$ into the second of Eqs. (A8) and make use of additional formulas for the elliptic integral of the third kind to be found on p. 13 of Ref. 28. We thus derive

$$M=(k/\tilde{\beta})^2(1-\tilde{\beta}^2)\left[1+\frac{k^2}{\tilde{\beta}^2-k^2}\coth^2(1/\lambda)\right]. \quad (17)$$

In Appendix C we find once more that $Q=1$ is the most stable state of all Q. Figure 3 demonstrates that, in addition to this, it is even more stable than the soliton lattice of case (a) with $Q=1$. Thus a new superlattice solution with a completely (n or p) filled localization band has been found. It is characterized by $\tilde{\beta}=1$, $M=0$, and $G=0$ for $0\le y\le 1/\cosh(1/\lambda)$. In spite of $Q=1$ it would probably not have been found without the expedient investigation of partially filled bands. From Eqs. (C1) and (C2) we infer

$$y=\frac{\tanh(1/\lambda)}{[k^2+\sinh^2(1/\lambda)]^{1/2}}\frac{\pi/2}{\Pi(-k^2/\sinh^2(1/\lambda),k)}, \quad (18)$$

$$W/N=-\frac{S}{4}\frac{\sinh^2(1/\lambda)}{k^2+\sinh^2(1/\lambda)}\tanh(1/\lambda)\times\left[\frac{K(k)}{\Pi(-k^2/\sinh^2(1/\lambda),k)}\right]^2.$$

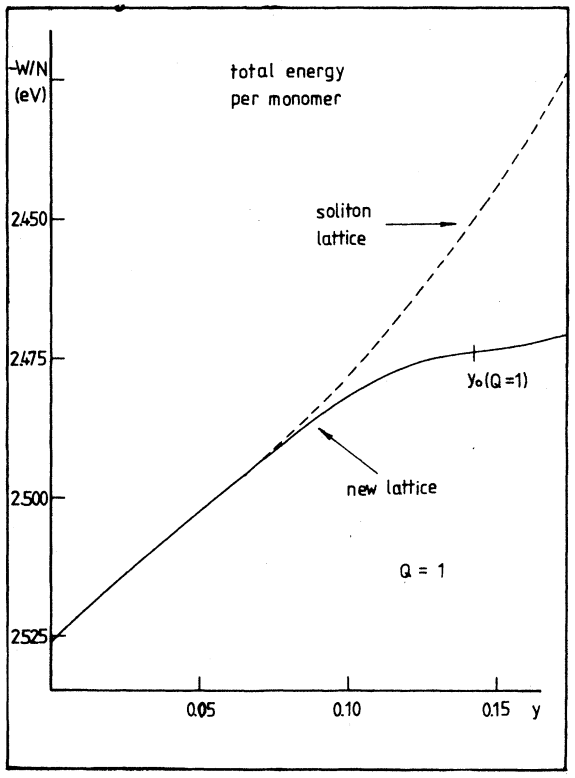

FIG. 3. Comparison between both superlattices. W/N vs y for $Q=1$. Soliton lattice (dashed line). New lattice (solid line). Proof that there exists a lattice more stable than the soliton lattice.

This is to be compared to Eqs. (14).

In contrast to Eq. (13), the lattice function of Eq. (4) reads

$$\tilde{\Delta}(x)=v_F\kappa\frac{\mathrm{sn}[\kappa(x-x_0),k]\,\mathrm{dn}[\kappa(x-x_0),k]}{\mathrm{cn}[\kappa(x-x_0),k]}$$

for $\kappa x\in\ldots,\ [-4K,-3K],\ [-2K,-K],\ [0,K],\ [2K,3K],\ \ldots$, with $x_0\kappa=K(k)/2$, and

$$\tilde{\Delta}(x)=-v_F\kappa\frac{\mathrm{sn}[\kappa(x-x_0),k]\,\mathrm{dn}[\kappa(x-x_0),k]}{\mathrm{cn}[\kappa(x-x_0),k]} \quad (19)$$

for $\kappa x\in\ldots,[-3K,-2K],\ [-K,0],\ [K,2K],\ [3K,4K],\ldots$, and $x_0\kappa=-K(k)/2$. It does not approach zero, but stays finite in the limit $k=0$.

Since the localized wave functions of Eqs. (17) of Ref. 20 must be treated with care in the limit $M=0$, we present them here. The phases of p_ν and q_ν differ by $\pi/2$; eigenvalue $E_\nu=0$ for all ν with $0\le|\nu|\le n/2$:

$$q_\nu(x)=\frac{ik}{\sqrt{2N}}\frac{\mathrm{cn}[\kappa x-K(k)/2,k]}{[E(k)/K(k)-(k')^2]^{1/2}},$$
$$p_\nu(x)=\frac{k}{\sqrt{2N}}\frac{\mathrm{cn}[\kappa x+K(k)/2,k}{[E(k)/K(k)-(k')^2]^{1/2}}. \quad (20)$$

Equations (1)–(3) of Ref. 20 can be shown to be satisfied. Note that the jumps in the derivative of $\tilde{\Delta}(x)$ near 0, $\pm K/\kappa,\ldots$ are without consequence, since in these equations only the continuous function $\tilde{\Delta}$ appears. As for wave functions and band energies of the extended states the limit $M=0$ in Eqs. (17) of Ref. 20 poses no problem. In Fig. 4 the new superlattices is compared to the soliton lattice. The zeros of $\tilde{\Delta}$ coincide with the maxima of the localized charge distribution functions, which also do not vanish in the limit $k=0$.

The boundaries of conduction and valence bands read [cf. Eq. (11)]

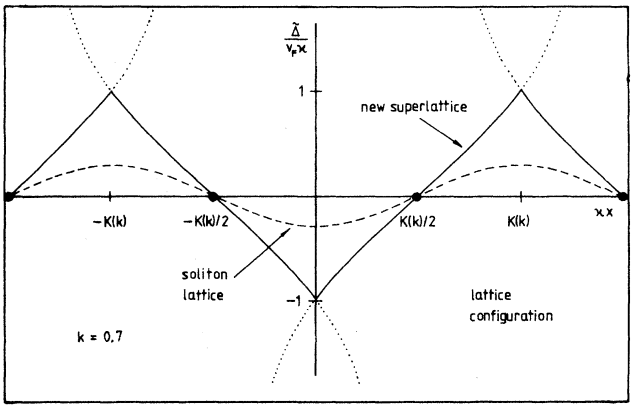

FIG. 4. Comparison between both superlattices. Lattice configuration function $\tilde{\Delta}$ depending on space coordinate x [cf. Eqs. (13) and (19)]. $k=0.7$. Distribution functions of localized charges (not shown) have maxima at zeros of $\tilde{\Delta}$. Soliton lattice (dashed line). New lattice (solid line). For clearness dotted lines show whole functions of Eq. (19), only parts of which are real. v_F is the Fermi velocity. For parameter $\kappa=2nK(k)/Na$, see text.

localized charge distribution functions, which also do not vanish in the limit $k=0$.

The boundaries of conduction and valence bands read [cf. Eq. (11)]

$$E_{l\,(u)}^{\text{cond (val)}} = \underset{(-)}{+}\, v_F \kappa k = \underset{(-)}{+}\, \frac{S}{\pi} y k K(k) \ . \tag{21}$$

In addition to these two bands there also exists a localization "band" in form of a δ function. From Eq. (10) we derive

$$\frac{N_C}{4N} Z^{\text{loc}}(E) = y\delta(E) \ ,$$

$$\frac{N_C}{4N} Z^{\text{ext}}(E) = \frac{1}{S} \frac{\varepsilon^2 + (k')^2 - E(k)/K(k)}{\{(\varepsilon^2 - k^2)[\varepsilon^2 + (k')^2]\}^{1/2}} \quad \text{for } |\varepsilon| > k \ . \tag{22}$$

Again $Z(E)$ is normalized to 1 as in Eq. (16) above. Figure 5 shows Z. It is clearly distinguished from Fig. 2. While the soliton midgap band is narrow only for small y and gets wider with increasing concentration, the central band of the new lattice is sharp for all $y \le 1/\cosh(1/\lambda)$ with weight y. At $k=0$ or $y=1/\cosh(1/\lambda)$ the function $Z^{\text{ext}}(E)$ changes its shape. Let us apply Eq. (22) to polyacetylene. Here $N_C/4N=1$ and $y=2y_D$. For $y \ge 1/\cos(1/\lambda)$ we have

$$Z^{\text{loc}}(E) = \frac{1}{\cosh(1/\lambda)} \delta(E) \ ,$$

$$Z^{\text{ext}}(E) = \frac{1}{S} \frac{|\varepsilon|}{(\varepsilon^2+1)^{1/2}}, \quad E = \frac{S}{2\cosh(1/\lambda)} \varepsilon \ . \tag{23}$$

Evidently for $0 \le y \le 1/\cosh(1/\lambda)$ the Fermi energy $E_F=0$. For larger y there is the equation

$$y = 1/\cosh(1/\lambda) + (2/S) \int_0^{E_F} dE \frac{\varepsilon}{(\varepsilon^2+1)^{1/2}}$$

or

$$E_F = \frac{S}{2} \left[y^2 - \frac{1}{\cosh^2(1/\lambda)} \right]^{1/2} \quad \text{for } y \ge \frac{1}{\cosh(1/\lambda)} \ . \tag{24}$$

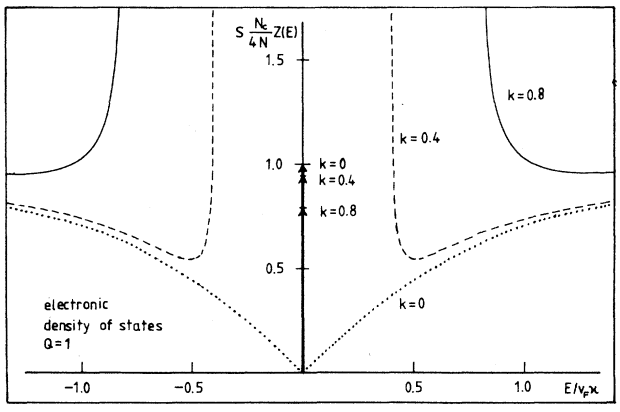

FIG. 5. Electronic density of states vs energy E for new superlattice with $Q=1$. Compare with Fig. 2. At $E=0$ a δ peak [cf. Eq. (23)]. Modulus $k=0.8$ (solid line); $k=0.4$ (dashed line); $k=0$ (dotted line). Weight of δ function taken from rest of curve.

We have anticipated that the number of localized charges does not increase on further doping and that more excess charges are stored in conducting states instead. The coexistence of localized and delocalized charges is to some extent reminiscent of the coexistence of condensate and excited particles in superfluid helium. For the density of states near the Fermi level we get

$$Z(E_F) = \frac{1}{S} \frac{\varepsilon_F}{(\varepsilon_F^2+1)^{1/2}} = \frac{1}{S} \left[1 - \frac{1}{[y\cosh(1/\lambda)]^2} \right]^{1/2} \ . \tag{25}$$

In the absence of any gap a tight-binding calculation in one dimension for a half-filled band of total width S would give $N_0 = 4/(\pi S)$ for the density of states at Fermi level. Using $\chi_P = \mu_B^2 Z(E_F)$ for the Pauli spin susceptibility, where μ_B is the Bohr magneton and $y=2y_D$, where y_D is the dopant concentration, we find

$$\chi_P = \frac{\pi}{4} N_0 \mu_B^2 \left[1 - \frac{1}{[2y_D\cosh(1/\lambda)]^2} \right]^{1/2}$$

$$\text{for } y_D \ge \frac{1}{2\cosh(1/\lambda)} \ . \tag{26}$$

Figure 6 shows χ_P for $\lambda=0.38$. The saturation value deviates from the "metallic" $N_0\mu_B^2$ by a factor of 0.8.

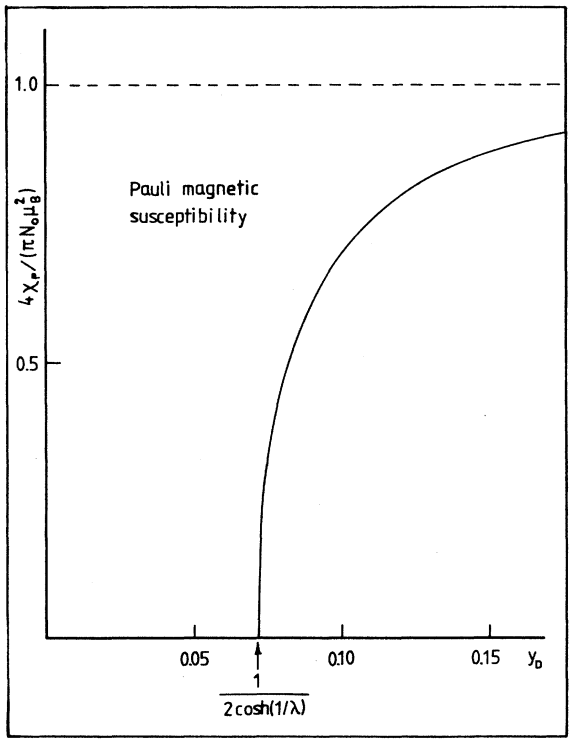

FIG. 6. Pauli spin susceptibility χ_P vs dopant concentration $y_D = y/2$ for *trans*-polyacetylene. Electron-phonon coupling constant $\lambda=0.38$. N_0 density of states at Fermi level for one dimensional metal. μ_B is the Bohr magneton.

V. DISCUSSION

The foregoing calculations have brought about three main results. First, regard the Pauli spin susceptibility of *trans*-polyacetylene. The observed sudden jump from very small to almost metallic values by more than 2 order of magnitude finds a simple explanation. The present (primitive) model yields a χ_P which starts from zero with infinite slope, then gradually approaches a saturation value, which is proportional to the reciprocal bandwidth $\sim 0.1/\text{eV}$ C-atom. Besides, the critical dopant concentration depends only on the electron-phonon coupling constant λ, giving about 7% for $\lambda=0.38$ independently of the dopant's nature. The soliton lattice does not show such an abrupt onset of χ_P. Experimentally the critical points scatter between 4% and 7% for dopants as iodine, sodium, ClO_4,AsF_5, etc. χ_P is not exactly zero before onset due to localized rest spins; its value is independent of concentration. The transitional regime seems to be a little smoothed, and the saturation value of χ_P for metallic concentrations is material dependent. These discrepancies may be attributed to three-dimensional Coulomb forces, electron-electron correlation, and disorder. Further refinement of the picture can be reached by taking into account possible reordering of the columns of dopants with different geometries.[29]

Second, there is an explanation for the band-gap closure observed at high doping level in optical-absorption[24] and electron-loss spectroscopy.[30] At low concentration the new superlattice and the soliton lattice are identical [cf. Eqs. (13) and (19)], showing the characteristic midgap absorption.[31–34] At higher concentrations they disagree. The interband gap of the soliton lattice widens, that of the new lattice narrows. The midgap band of the soliton lattice increased in width, that of the new lattice stays sharp. Its gap vanishes at about 7% doping, while for the soliton lattice the two gaps between midband and extended bands are not closed before maximal doping. The experimental situation is not unique insofar as evidence for gap broadening has been claimed to be seen,[35] which would point to a soliton lattice. Since the energy difference between both lattice forms is small, there might be a chance to observe either of them in dependence on the actual situation. In any case, the optical absorption due to the new lattice should first be computed.

Third, experimentally the infrared modes induced by doping persist into the metallic region, remaining even at the highest dopant concentration, which implies that the metallic state is not a uniform bond-length polymer but one with structural distortion. This observation favors the new superlattice form, because this is exactly what happens in it. At the transition point the lattice function $\tilde{\Delta}$ and the localized charge-distribution functions do not vanish but survive instead, independent of how large the dopant concentration is. We have a gapless metallic state in combination with a distorted lattice and localized charges. The soliton lattice has quite different features, since lattice distortion and charge localization are gradually diminished on doping.

The above results only apply if dopants are uniformly distributed, which is signaled by the sharpness of the transition. This is important, because randomness of the doping process has also been made responsible for a semiconductor-metal transition.[36,37] Hence the influence of sample preparation must not be forgotten. The Coulomb potential of dopant ions has been shown[29] to be of possible importance for the reduction of level spacing, redistribution of gap states, and gap filling. Other effects already mentioned can be taken into consideration by way of perturbational methods. For the calculation of thermopower and heat capacity, the above calculations have to be modified to include temperature dependence.

It will be important to know whether the new lattice is also present in the discrete SSH model, which until now has not yet been shown. Since one has to proceed numerically with a variational calculus, the energy difference between both competing lattices should be sufficiently large to ensure convergence. In Fig. 3, however, it is shown that for small concentrations the energies of both lattices practically agree. Hence we need large concentrations y near 14%. From Ref. 20 it has become clear that in the case of finite chain lengths the monomer numer N must exceed a certain value to guarantee a stable solution, which in our case is between 200 and 300 monomers. Thus numerical variation should be performed on chains with more than 600 carbon atoms in contrast to the 100 or less C atoms usually considered.

Another interesting point is the question of what happens to the new solution if the confinement parameter deviates somewhat from zero. This is, in fact, the case with realistic polyacetylene. If the new lattice is not to be a mere artifact, Eqs. (A8) should be investigated in general with varying confinement parameters.

ACKNOWLEDGMENTS

It is a pleasure to thank Professor H. Schmidt, Professor H. Heyszenau, and Dr. P. Hertel for valuable discussions on the subject of the coexistence of localized and delocalized electronic states. This work has been supported by a grant from the Deutsche Forschungsgemeinschaft (Bonn, West Germany).

APPENDIX A

For further advance, elliptic integrals of all kinds, complete and incomplete, are required.[28] To prevent misunderstanding, we summarize here their definitions:

$$\begin{aligned}
&\Pi(\varphi,\alpha^2,k)=\int_0^{\varphi} d\tau \frac{1}{(1-\alpha^2\sin^2\tau)(1-k^2\sin^2\tau)^{1/2}}\ ,\\
&F(\varphi,k)=\Pi(\varphi,\alpha^2=0,k)\ ,\\
&E(\varphi,k)=\int_0^{\varphi} d\tau (1-k^2\sin^2\tau)^{1/2}\ ,\\
&\Pi(\alpha^2,k)=\Pi(\varphi=\pi/2,\alpha^2,k)\ ,\\
&K(k)=F(\varphi=\pi/2,k)\ ,\\
&E(k)=E(\varphi=\pi/2,k)\ .
\end{aligned} \tag{A1}$$

These functions allow Eqs. (1) to be treated analytically. The intermediary mathematical steps can be found in Ref. 28. Several variable transformations are performed, the first of which [from ν to α_ν or β_ν with the help of Eqs. (17) of Ref. 20] means a substitution of phase shifts for wave numbers:

$$\frac{\pi}{n}\int_{n/2}^{N/2} d\nu\, f(1/\alpha_\nu^2)=\int_{\alpha_1}^{\alpha_2} f(1/\alpha^2)d\left[\left[\frac{(1+\alpha^2)(k^2+\alpha^2)}{\alpha^2}\right]^{1/2}\Pi(-\alpha^2,k)\right]$$
$$=\int_{z_1}^{z_2} f(z^2)d\left[\left[\frac{(1+z^2)(1+k^2z^2)}{z^2}\right]^{1/2}\Pi(-1/z^2,k)\right]=\int_{z_1}^{z_2} dz\, f(z^2)\frac{K(1+k^2z^2)-E}{[(1+z^2)(1+k^2z^2)]^{1/2}}\ . \quad \text{(A2)}$$

In the last step replace z by γ via

$$z=(1+k^2/M)^{1/2}\sin(\gamma)[1-(1+k^2/M)\sin^2\gamma]^{-1/2}\ . \quad \text{(A3)}$$

Evaluation of the other integral proceeds in a similar manner

$$\frac{\pi}{n}\int_{Qn/2}^{n/2} d\nu\, f(1/\beta_\nu^2)=\frac{\pi}{2}\int_{\tilde\beta}^{1} f(1/\beta^2)d\left[\Lambda_0\left[\sin^{-1}\left[\frac{\beta^2-k^2}{\beta^2(1-k^2)}\right]^{1/2},k\right]\right]$$
$$=\frac{\pi}{2}\int_{1/\tilde\beta}^{1} f(z^2)d\left[\Lambda_0\left[\sin^{-1}\left[\frac{1-k^2z^2}{1-k^2}\right]^{1/2},k\right]\right]=\int_{1}^{1/\tilde\beta} dz\, f(z^2)\frac{E-(1-k^2z^2)K}{[(z^2-1)(1-k^2z^2)]^{1/2}}\ . \quad \text{(A4)}$$

This time make the substitution

$$z=[1-(1-k^2)\sin^2\gamma]^{-1/2}\ . \quad \text{(A5)}$$

Λ_0 is Heuman's lambda function.[28] The integral boundaries z_1, z_2, and $\tilde\beta$ are determined by

$$\frac{\pi}{2}=\left[\frac{(1+z_1^2)(1+k^2z_1^2)}{z_1^2}\right]^{1/2}\Pi(-1/z_1^2,k)\ ,$$
$$\frac{\pi}{2}\frac{1}{c}=\left[\frac{(1+z_2^2)(1+k^2z_2^2)}{z_2^2}\right]^{1/2}\Pi(-1/z_2^2,k)\ , \quad \text{(A6)}$$
$$Q=\Lambda_0\left[\sin^{-1}\left[\frac{\tilde\beta^2-k^2}{\tilde\beta^2(1-k^2)}\right]^{1/2},k\right]\ .$$

Solution of the first equation immediately yields $z_1=0$. It turns out that another auxiliary parameter X is more suitable than z_2:

$$X=z_2/[(1+z_2^2)(1+k^2/M)]^{1/2}\ . \quad \text{(A7)}$$

Equations (1), (2), and (A6) ultimately lead to the following set of coupled equations, where $k'=(1-k^2)^{1/2}$:

$$Q=\Lambda_0\left[\sin^{-1}\left[\frac{\tilde\beta^2-k^2}{\tilde\beta^2(1-k^2)}\right]^{1/2},k\right]\ ,$$
$$\frac{1}{\lambda}=\sqrt{M}\left[F(\sin^{-1}X,k'(1+k^2/M)^{1/2})-F\left[\sin^{-1}\left[\frac{1-\tilde\beta^2}{1-k^2}\right]^{1/2},k'(1+k^2/M)^{1/2}\right]\right]$$
$$+\frac{k^2}{\sqrt{M}}\left[\Pi\left[\sin^{-1}\left[\frac{1-\tilde\beta^2}{1-k^2}\right]^{1/2},(k')^2,k'(1+k^2/M)^{1/2}\right]-F\left[\sin^{-1}\left[\frac{1-\tilde\beta^2}{1-k^2}\right]^{1/2},k'(1+k^2/M)^{1/2}\right]\right]$$
$$+\frac{k^2}{\sqrt{M}}\Pi(\sin^{-1}X,1+k^2/M,k'(1+k^2/M)^{1/2})\ , \quad \text{(A8)}$$
$$\frac{\lambda S}{2\Delta}(M+k^2-1)^{1/2}\left[F(\sin^{-1}X,k'(1+k^2/M)^{1/2})-F\left[\sin^{-1}\left[\frac{1-\tilde\beta^2}{1-k^2}\right]^{1/2},k'(1+k^2/M)^{1/2}\right]\right]$$
$$=\frac{\sqrt{M}}{M+k^2}\left[\frac{1-(k')^2X^2(1+k^2/M)}{X^2[1-X^2(1+k^2/M)]}\right]^{1/2}\frac{1}{K(k)}\Pi(1-1/[X^2(1+k^2/M)],k)\ ,$$
$$G=\frac{2\Delta}{\lambda\sqrt{M}}\Big/\left[F(\sin^{-1}X,k'(1+k^2/M)^{1/2})-F\left[\sin^{-1}\left[\frac{1-\tilde\beta^2}{1-k^2}\right]^{1/2},k'(1+k^2/M)^{1/2}\right]\right]\ ,$$
$$c=\frac{\pi G}{2SK(k)}\left[\frac{M}{(M+k^2)(M+k^2-1)}\right]^{1/2}\ .$$

When solving Eqs. (A8) we do not start with the concentration c, but proceed the opposite way. λ, Δ, S, and Q are fixed constants. We pick a value for k from the interval (0,1), solve the first equation to get $\tilde{\beta}$, then the coupled second and third equations for M and X. G and c follow in return from the last two equations. Wave functions and band energies are given by Eqs. (17) of Ref. 20 in terms of these variables. Then electronic densities of states and transition matrix elements can be derived.

APPENDIX B

After insertion of $M=1-k^2$ into the second of Eqs. (A8), we get[28]

$$X=k'\tanh(1/\lambda_0)\ ,$$
$$\frac{1}{\lambda_0}=\frac{1}{\lambda}+\ln\left[\frac{1+(1-\tilde{\beta}^2)^{1/2}}{1-(1-\tilde{\beta}^2)^{1/2}}\right]^{1/2}. \tag{B1}$$

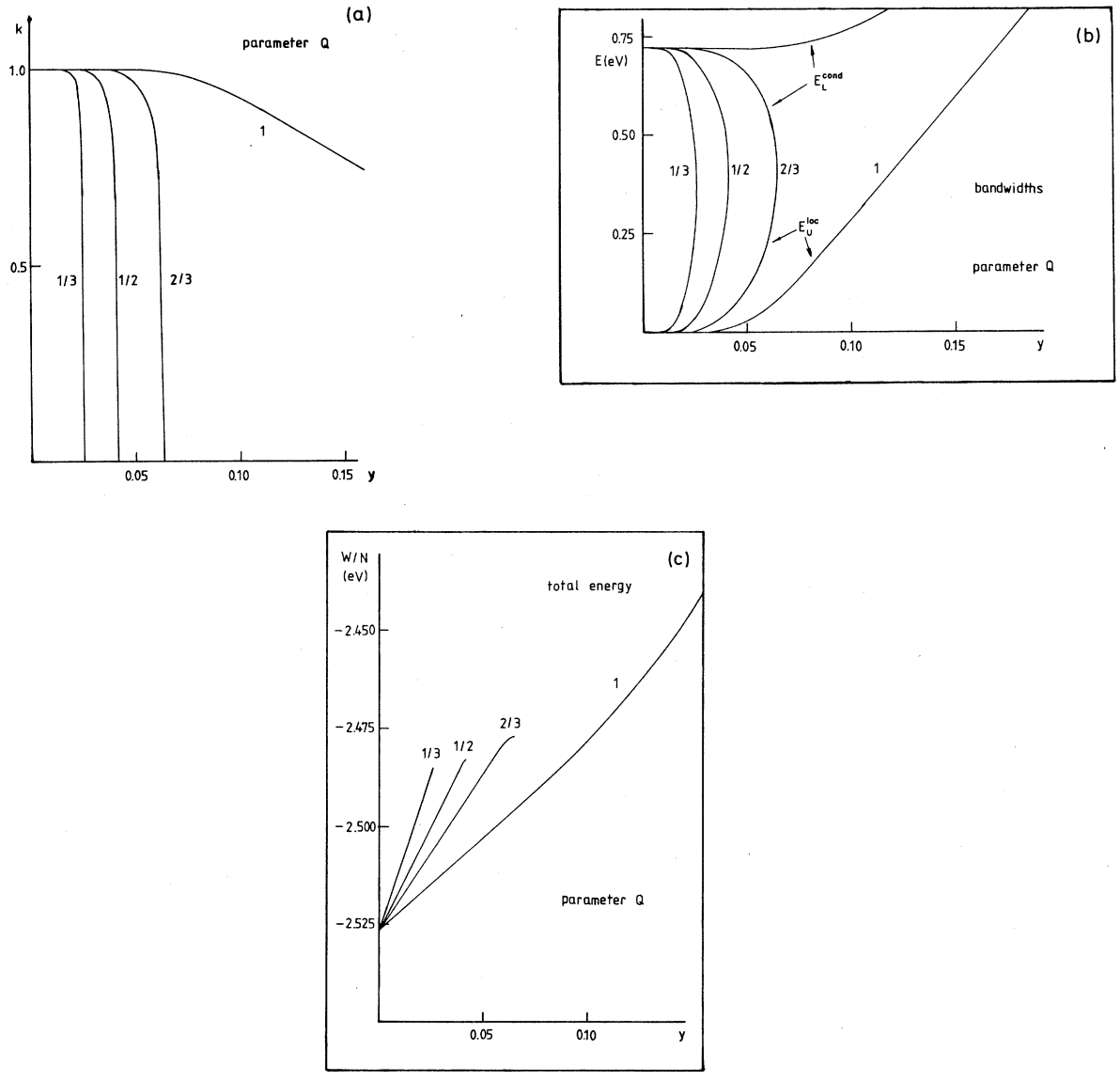

FIG. 7. Soliton lattice for confinement parameter $\Delta=0$ and electron-phonon coupling $\lambda=0.38$ with partially filled localization band. (a) Modulus k vs concentration $y=Qn/N=n'/N=$number of charge pairs divided by monomer number for varying Q. $k=1$: soliton lattice exists. $k=0$: soliton lattice vanishes at $y_0=Q\,[1+(1-Q^2)\exp(2/\lambda)]^{-1/2}$. For $y>y_0$ there is $k=0$. (b) y dependence of bandwidths for positive energy E; mirror images for $E<0$. Q varies as in a. Gap between midband and conduction band closed at the same y_0 as appears in (a). (c) Total energy (lattice plus electronic) per monomer W/N vs y for Q varying. Curves valid for $y<y_0$. $Q=1$ denotes most stable lattice with full (or empty) midgap band.

Inserting the third into the fourth, and the fourth into the fifth of Eqs. (A8), we recover a relation between $c=n/N$ and modulus k:

$$c=\frac{(\pi/2)\tanh(1/\lambda_0)}{[1+k^2\sinh^2(1/\lambda_0)]^{1/2}\Pi(-1/\sinh^2(1/\lambda_0),k)}\,. \tag{B2}$$

From Eq. (7) we finally obtain for the total energy

$$W/N=-\frac{S}{4}\frac{k^2\sinh^2(1/\lambda_0)}{1+k^2\sinh^2(1/\lambda_0)}\tanh(1/\lambda_0)\times\left[\frac{K(k)}{\Pi(-1/\sinh^2(1/\lambda_0),k)}\right]^2. \tag{B3}$$

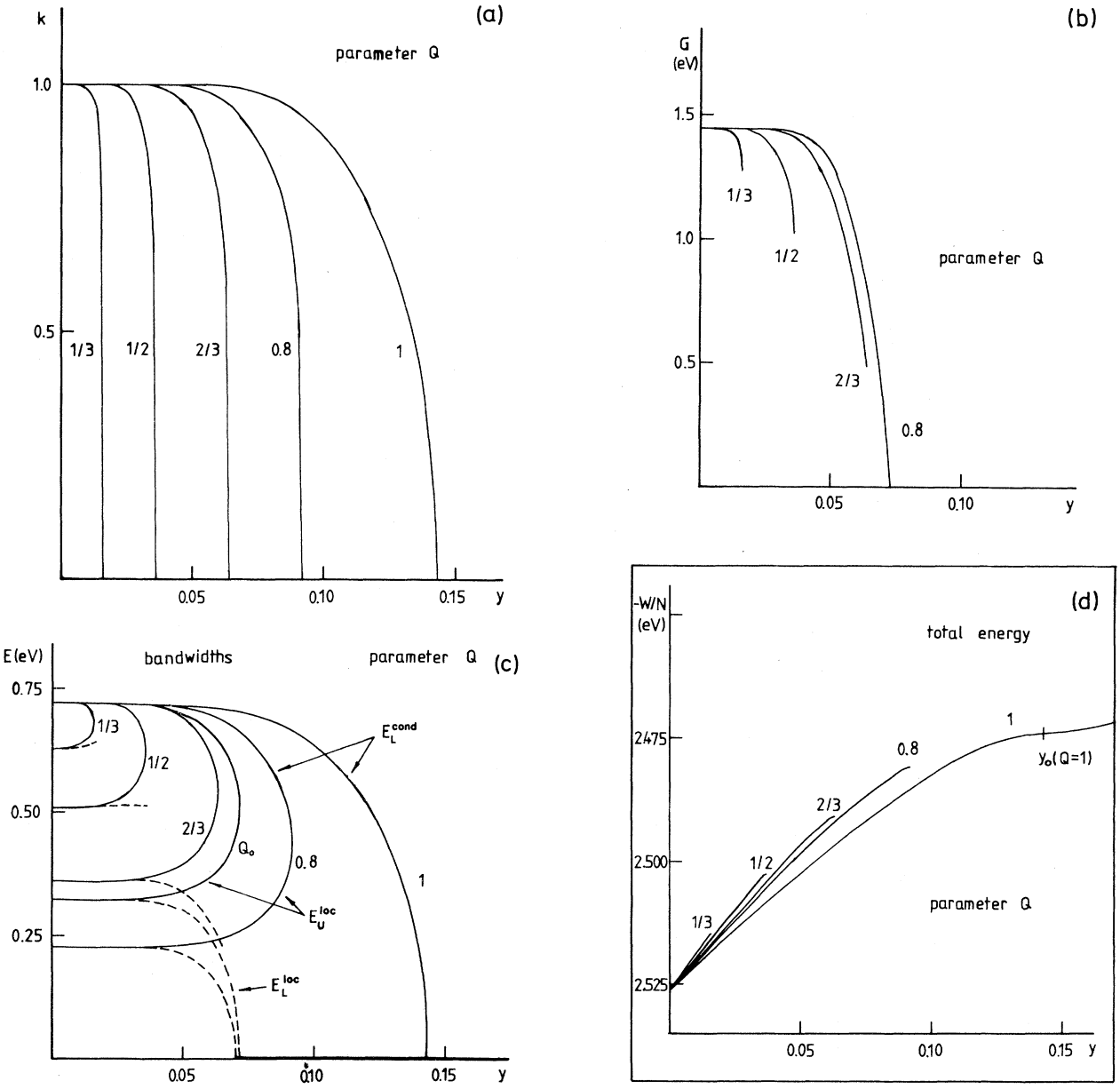

FIG. 8. New superlattice for confinement parameter $\Delta=0$ and electron-phonon coupling constant $\lambda=0.38$ with partially filled localization band. Compare with Fig. 7. (a) Modulus k vs y for various Q. k vanishes for $y_0=Q^2/\cosh(1/\lambda)$. y_0 maximal for $Q=1$. Lattice configuration does not go to zero here (see text). (b) Gap parameter G vs y for different Q. For y_0 (or $k=0$) G is identical to the central gap. At $k=0$ G vanishes for $Q\geq Q_0=\{[1+\exp(-2/\lambda)]/2\}^{1/2}$. (c) Band edges for $E>0$ with varying Q in dependence on y. Same picture for $E<0$ with mirror plane at $E=0$. At y_0 the gap between conduction and localization band is closed. At y_0 with $Q=Q_0$ the central gap vanishes. For larger Q, the part with $G=0$ ($E_l^{\rm loc}=0$) increases. At $Q=1$ there is $G\equiv 0$. (d) Total energy W/N vs y. Parameter Q. Range of validity $y\leq y_0=Q^2/\cosh(1/\lambda)$. $Q=1$ most stable: midgap band also full or empty for new superlattice.

k given variation of Q in the first of Eqs. (A8) yields $\tilde{\beta}$. Afterwards λ_0 is taken from Eq. (B1).

Figure 7 shows modification of modulus k, bandwidths, and total energy W/N with $y=Qc$, where $0\le y\le Q$. Note that k approaches zero at $y_0=Q[1+(1-Q^2)\exp(2/\lambda)]^{-1/2}\le Q$. At this point the gap between localization and conduction bands vanishes. From Fig. 7(c) we infer, however, that the most stable state corresponds to $Q=1$ with $\lambda_0=\lambda$. This is not new,[18] since the midgap band of a stable charged soliton lattice is completely n or p filled. For that case $y_0=1$, i.e., gap closure does not take place in our model before maximal doping.

APPENDIX C

By combination of the last three of Eqs. (A8) we get a relationship between c and k:

$$c=\left[\frac{k^2(1-\tilde{\beta}^2)+(k')^2\tilde{\beta}^2\sinh^2(1/\lambda)}{k^2+\tilde{\beta}^2\sinh^2(1/\lambda)}\right]^{1/2}\frac{(\pi/2)(\tilde{\beta}^2-k^2)^{1/2}[\tilde{\beta}(k')^2\cosh(1/\lambda)]}{\Pi(-k^2(\tilde{\beta}^2-k^2)/[k^2(1-\tilde{\beta}^2)+(k')^2\tilde{\beta}^2\sinh^2(1/\lambda)],k)},$$
$$G=\frac{2S}{\pi}cK(k)\left[\frac{(M+k^2)(M+k^2-1)}{M}\right]^{1/2}. \tag{C1}$$

Finally, from Eq. (7),

$$\frac{W}{N}=-\frac{S}{4}\frac{[k^2(1-\tilde{\beta}^2)+\tilde{\beta}^2(k')^2\sinh^2(1/\lambda)][k^4(1-\tilde{\beta}^2)+\tilde{\beta}^4(k')^2\sinh^2(1/\lambda)]}{\tilde{\beta}^4(k')^4\sinh(1/\lambda)\cosh(1/\lambda)[k^2+\tilde{\beta}^2\sinh^2(1/\lambda)]}\times\left[\frac{K(k)}{\Pi(-k^2(\tilde{\beta}^2-k^2)/[k^2(1-\tilde{\beta}^2)+\tilde{\beta}^2(k')^2\sinh^2(1/\lambda)],k)}\right]^2. \tag{C2}$$

Figure 8 shows k, G, band edges, and W/N versus $y=cQ$ for various Q. k drops to zero at $y_0=Q^2/\cosh(1/\lambda)<Q$. Here the gap between upper localization and conduction bands and the symmetrically positioned gap for negative energy are closed. The central gap is still present and coincides with G for $k=0$. It goes to zero at $Q_0=\{[1+\exp(-2/\lambda)]/2\}^{1/2}$. Again $Q=1$ corresponds to the most stable state.

[1] S. A. Brazovskii, Pis'ma Zh. Eksp. Teor. Fiz. **28**, 656 (1978) [JETP Lett. **28**, 606 (1978)].

[2] W. P. Su, J. R. Schrieffer, and A. J. Heeger, Phys. Rev. Lett. **42**, 1698 (1979).

[3] W. P. Su and J. R. Schrieffer, Proc. Nat. Acad. Sci. U.S.A. **77**, 5526 (1980).

[4] D. K. Campbell and A. R. Bishop, Phys. Rev. B **24**, 4859 (1981).

[5] A. R. Bishop and D. K. Campbell, in *Nonlinear Problems: Present and Future*, edited by A. R. Bishop, D. K. Campbell, and B. Nicolaenko (North-Holland, Amsterdam, 1982), p. 195.

[6] Y. Onodera, Phys. Rev. B **30**, 775 (1984).

[7] W. P. Su, J. R. Schrieffer, and A. J. Heeger, Phys. Rev. B **22**, 2099 (1980); **28**, 1138(E) (1983).

[8] H. Takayama, Y. R. Lin-Liu, and K. Maki, Phys. Rev. B **21**, 2388 (1980).

[9] S. A. Brazovskii and N. N. Kirova, Pis'ma Zh. Eksp. Teor. Fiz. **33**, 6 (1981) [JETP Lett. **33**, 4 (1981)].

[10] R. R. Chance, D. S. Boudreaux, J. L. Brédas, and R. Silbey, in *Handbook of Conducting Polymers*, edited by T. A. Skotheim (Dekker, New York, 1986), Vol. 2, p. 825.

[11] J. L. Brédas, in Ref. 10, p. 859.

[12] R. L. Elsenbaumer and L. W. Shacklette, in *Handbook of Conducting Polymers*, edited by T. A. Skotheim (Dekker, New York, 1986), Vol. 1 p. 213.

[13] G. B. Street, in Ref. 12, p. 265.

[14] G. Tourillon, in Ref. 12, p. 293.

[15] R. H. Baughman, L. W. Shacklette, N. S. Murthy, G. G. Miller, and R. L. Elsenbaumer, Mol. Cryst. Liq. Cryst. **118**, 253 (1985).

[16] M. Winokur, Y. B. Moon, A. J. Heeger, J. Barker, D. C. Bott, and H. Shirakawa, Phys. Rev. Lett. **58**, 2329 (1987).

[17] S. A. Brazovskii, S. A. Gordyunin, and N. N. Kirova, Pis'ma Zh. Eksp. Teor. Fiz. **31**, 486 (1980) [JETP Lett. **31**, 456 (1980)].

[18] B. Horovitz, Phys. Rev. Lett. **46**, 742 (1981); Phys. Rev. B **35**, 734 (1987).

[19] A. Saxena and J. D. Gunton, Phys. Rev. B **35**, 3914 (1987).

[20] M. Dinter, Phys. Rev. B **36**, 9628 (1987).

[21] P. Bernier, in *Handbook of Conducting Polymers*, edited by T. A. Skotheim (Dekker, New York, 1986), Vol. 2, p. 1099.

[22] F. Moraes, J. Chen, T. C. Chung, and A. J. Heeger, Synth. Met. **11**, 271 (1985); Solid State Commun. **53**, 757 (1985).

[23] K. Mizoguchi, K. Misoo, K. Kume, K. Kaneto, T. Shiraishi, and K. Yoshino, in *Abstracts of the International Conference on Science and Technology of Synthetic Metals, Kyoto, 1986*, edited by H. Shirakawa, T. Yamabe, and K. Yoshino [Synth. Met. **17-19**, 221 (1987)].

[24] X. Q. Yang, D. B. Tanner, M. J. Rice, H. W. Gibson, A. Feldblum, and A. J. Epstein, Solid State Commun. **61**, 335 (1987).

[25] D. Tanner, G. Doll, K. Rao, M. H. Yang, P. C. Eklund, G. Arbuckle, and A. G. MacDiarmid, Bull. Am. Phys. Soc. **32**, 422 (1987).

[26]S. Kivelson and A. J. Heeger, Phys. Rev. Lett. **55**, 308 (1985); Synth. Met. **17**, 183 (1987).
[27]H. Y. Choi and E. J. Mele, Phys. Rev. B **34**, 8750 (1986).
[28]P. F. Byrd and M. D. Friedman, *Handbook of Elliptic Integrals for Engineers and Scientists* (Springer, Berlin, 1971).
[29]E. M. Conwell and S. Jeyadev, Phys. Rev. Lett. **61**, 361 (1988).
[30]G. Crecelius, in *Handbook of Conducting Polymers,* edited by T. A. Skotheim (Dekker, New York, 1986), Vol. 2, p. 1233.
[31]*Proceedings of the International Conference on the Physics and Chemistry of Low Dimensional Synthetic Metals, Abano, Terme, 1984* [Mol. Cryst. Liq. Cryst. **117-121**, (1985)].
[32]J. Tanaka and M. Tanaka, in *Handbook of Conducting Polymers,* edited by T. A. Skotheim (Dekker, New York, 1986), Vol. 2, p. 1269.
[33]S. Jeyadev and E. M. Conwell, Phys. Rev. B **33**, 2530 (1986).
[34]J. Tinka Gammel, Phys. Rev. B **37**, 6517 (1988).
[35]E. Ehrenfreund, Z. Vardeny, O. Brafman, R. Weagley, and A. J. Epstein, Phys. Rev. Lett. **57**, 2081 (1986).
[36]E. J. Mele and M. J. Rice, Phys. Rev. B **23**, 5397 (1981).
[37]W. P. Su, Solid State Commun. **47**, 947 (1983).